PHILOSOPHICAL TRANSACTIONS OF THE ROYAL SOCIETY A
MATHEMATICAL, PHYSICAL & ENGINEERING SCIENCES

The Application of Intense Ion Beams to the Creation of Hot Dense Plasmas [and Discussion]

T. D. Beynon and A. C. Walker

Phil. Trans. R. Soc. Lond. A 1981 **300**, 613-621
doi: 10.1098/rsta.1981.0089

Phil. Trans. R. Soc. Lond. A **300**, 613–621 (1981) [613]
Printed in Great Britain

The application of intense ion beams to the creation of hot dense plasmas

By T. D. Beynon
*Department of Physics, University of Birmingham, Birmingham B*15 2*TT, U.K.*

A broad review is presented of the physics central to the production of hot dense plasmas by intense ion beams. Particular attention is paid to the reasons for using ion beams rather than lasers. By using simple laws the required beam intensities and ion energies for light ions (protons, deuterons, etc.) and heavy ions ($A \gtrsim 120$) are compared. Current understanding of ion-dense plasma interactions is discussed together with current thinking on possible accelerator sources of intense beams and their final transport to small targets. Emphasis is placed throughout on the use of ion beams for heating targets of deuterium–tritium mixtures to thermonuclear ignition.

1. Introduction

The creation of hot dense plasmas by thermally driven shock waves is a subject which has received considerable attention over the past three or four decades, mainly in the field of weapons design. Much of the current interest in the creation of hot ($T \gtrsim 10\,\text{keV}$) dense ($\rho \approx 300\,\text{g/cm}^3$) plasmas is aimed at producing thermonuclear ignition of deuterium–tritium mixtures in micropellet targets with the ultimate goal of building economically viable civilian power stations. Conceptual studies have concentrated on powerful lasers, accelerators of beams of energetic ions, relativistic high current electron beams and macroparticle accelerators as possible drivers for inertial confinement fusion (i.c.f.) systems. In this paper I shall attempt to answer three questions central to the use of energetic ion beams. First, why use ions? Secondly, what is our understanding of ion–plasma interaction physics? Finally, how can these energetic ion beams be produced and focused on a target of dimensions of about a millimetre?

2. Some general considerations

2.1. *Choice of driver system*

Suppose we consider the overall energy balance in a conceptual energy-producing plant as in figure 1, where the following definitions have been used:

η_D efficiency of driver system (laser, accelerator, etc.);
G total gain of target pellet and reactor system ($G = G_P G_R$);
G_P pellet gain (pellet energy yield/beam energy incident from driver);
G_R reactor system gain due to exoergic nuclear reactions in reactor blanket;
η_P thermal-to-electric conversion efficiency of plant;
i_o net output of energy.

Since $G\eta_D\eta_P i_r = i_o + i_r$, the requirement that $i_o/i_r > 1$ demands that $G_P\eta_D > 2/G_R\eta_P$. Putting $G_R \approx 1.2$ and $\eta_P \approx \frac{1}{3}$ we obtain the condition that $G_P\eta_D > 5$. For laser-driven systems the most favourable estimates of efficiencies are about 5% for CO_2 and KrF lasers while for ion accelerators, particularly for heavy ions, efficiencies of at least 25% can be expected. Thus for an ion-driven system the high-gain requirements of a target can be reduced by a factor of at least five compared with the best laser-driven system. The relatively high efficiency of ion accelerators is therefore the most important fundamental reason for the choice of ions as target drivers.

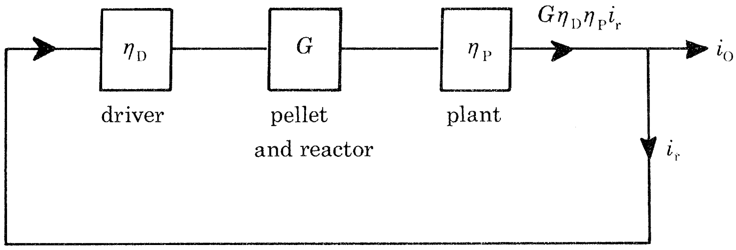

FIGURE 1. Schematic outlay of a driver system (laser, accelerator), a pellet and reactor system, and an energy conversion plant.

2.2. *Simple scaling laws*

As detailed hydrodynamic studies of a variety of spherical target designs become more refined a number of theoretical requirements are being established. One is that to achieve central ignition of a solid deuterium–tritium mixture in a pellet of radius of a few millimetres, an energy of about 20–30 MJ/g must be deposited in the target in about 10 ns to achieve a significant gain, a result which is largely independent of the detailed nature of the energy deposition process. We can use this result to obtain an approximate scaling law. A spherical shell, radius r, thickness Δr, and density ρ, is assumed to stop an ion beam of ions mass M_i, stripped charge state Z_i and energy E_i. Since the ions lose their energy predominantly by Coulomb interactions with the electrons in the region Δr we can put for the ions

$$\frac{dE}{dx} \approx -\frac{4\pi N Z_i^2 e^4 M_i}{2mE_i} \ln \Omega, \tag{1}$$

where m is the electron mass, and N is the electron number density.

Integrating (1), by assuming approximate constancy of the Coulomb logarithm $\ln \Omega$, gives the approximate ion range λ as

$$\lambda \approx mE_i^2/4\pi N Z_i^2 e^4 M_i \ln \Omega = \Delta r. \tag{2}$$

The specific energy deposition, ϵ_d, obtained by assuming that most of the target mass is in the shell Δr, is

$$\epsilon_d = nN_i E_i/4\pi r^2 \lambda\rho \approx \text{const.}, \tag{3}$$

where N_i is the total number of ions of energy E_i in n beams entering and stopping in the spherical annulus in a pulse length Δt. For a current I in each beam $N_i = I\Delta t/Z_i' e$, where Z_i' is the ion charge state in the beam. Putting $\rho \propto N$ and using (2) in (3) gives the following approximate scaling law:

$$nIM_i Z_i^2 \Delta t/r^2 E_i Z_i' \approx \text{const.} \tag{4}$$

A typical energy requirement for a well designed target is about 5 MJ in about 10 ns, representing a mean power level on the target of about 5×10^{14} W. For a 10 GeV ion in a charge state 2+ this is equivalent to a beam current of 10^5 A. If we assume that this target is designed for 10 GeV U^{2+} ions which will have, say, a mean stripped charge state of $Z_i \approx 80+$ during slowing down, equation (4) indicates that a target of the same size and performance would require a beam current of order of magnitude several hundred megamps of 100 MeV protons. Equation (4), although approximate, gives us the magnitude of the scaling required for moving from low currents of highly energetic heavy ions to high currents of less energetic light ions and illustrates the importance of the effective charge state Z_i, a point discussed later. It is also worth noting that this current of 10^5 A of U^{2+} ions would deliver only 3×10^{15} particles into the target.

3. Interactions of intense ion beams with a plasma

3.1. *Some general comments*

The problem to be considered is that of a beam of energetic ions focused to about 1 mm beam-width on a medium or high-Z material which is initially cold but which may attain a temperature of about 100 eV in the duration of the beam pulse. A beam of 10 GeV ions of mass 200 u (u $\approx$ 1.661 $\times 10^{-27}$ kg) focused down to 10^{14} W cm^{-2} will have an ion density of 2×10^{14} cm^{-3} while a similar beam of 100 MeV protons will have a density of 1.4×10^{16} cm^{-3}, corresponding to particle mean spacings of 1.7×10^{-5} cm and 4.1×10^{-6} cm respectively. A target of solid material at 200 eV corresponding to an electron density of 10^{23} cm^{-3} has a Debye length λ_D ($\lambda_D = kT/4\pi Ne^2$) of 2.3×10^{-8} cm. Particles in the beam can therefore safely be treated as independent 'test particles' in their behaviour in the plasma. Additionally, we can to a good approximation ignore multiple scattering effects and treat the ions as moving in straight lines, so that specific energy deposition rates $\mathrm{d}\epsilon(\boldsymbol{r})/\mathrm{d}t$ at a position $\boldsymbol{r}$ in the target can be computed as

$$\mathrm{d}\epsilon(\boldsymbol{r})/\mathrm{d}t = v_i f(\boldsymbol{r})\, S(E_i),$$

where v_i is the velocity, $S(E_i)$ is the slowing-down power and $f(\boldsymbol{r})$ is the geometric form factor for the target.

Interactions of the projectile ion in the plasma may be divided into three broad categories:

(i) elastic Coulomb interactions with the electrons (bound and free) and the ions in the plasma;
(ii) inelastic electromagnetic interactions giving rise to bremsstrahlung, pair production and pion production;
(iii) hadronic interactions via the strong nuclear force, producing in particular fission fragments.

Additionally, possible effects of the finite size of the projectile ion and the important problem of the effective charge state of the projectile ion in the plasma need to be considered. We should recall that our energy/mass ratios, E_i/M_i, are such that $E_i/M_i \lesssim 100$ MeV/u with the corresponding relativistic parameters $\beta \lesssim 0.45$ and $\gamma = (1-\beta^2)^{-\frac{1}{2}} \lesssim 1.12$.

3.2. *Elastic Coulomb interactions*

Many reviews have appeared in the literature on the theory of charged particle penetration in cold matter (Rossi 1952; Bethe & Ashkin 1953; Allison & Warshaw 1953; Uehling 1954; Landau & Lifshitz 1960; Fano 1963; Northcliffe 1963; Bichsel 1968, 1972; Jackson 1975) and in completely ionized plasmas (Lindhard 1954; Butler & Buckingham 1962; Longmire 1963; Sigmar & Joyce 1971). The problem now under consideration is that of calculating the stopping power $S(E_i)$ in a partially ionized plasma where the degree of ionization is increasing with the temperature increase. For high-Z materials only 40–50 % of the material may be ionized.

PHILOSOPHICAL TRANSACTIONS OF THE ROYAL SOCIETY A MATHEMATICAL, PHYSICAL & ENGINEERING SCIENCES

The bound-electron component $S_b(E_i)$ of the total slowing-down power can be obtained from the corrected Bethe–Fano formula (Sternheimer 1956; Fano 1963):

$$S_b(E_i) = (\omega_p^2 Z_i^2 e^2/v_i^2)\{\ln(2mv_i^2/I) - \ln(1-\beta^2) - \beta^2 - \tfrac{1}{2}\delta - C/Z_2\} \quad (5)$$

where

$$\ln I = \sum_n fn \ln\{h\omega_n(1+\omega_p^2 fn/\omega_n^2)^{\frac{1}{2}}\},$$

$$\delta = \sum_n fn \ln\left(1+\frac{\theta^2}{\omega_n^2}\right) - (1-\beta^2)\frac{\theta^2}{\omega_p^2},$$

$$\theta = \omega(0)/i,$$

$$\omega^2(q)\{\epsilon(\omega(q)) - \beta^{-2}\} = c^2q^2,$$

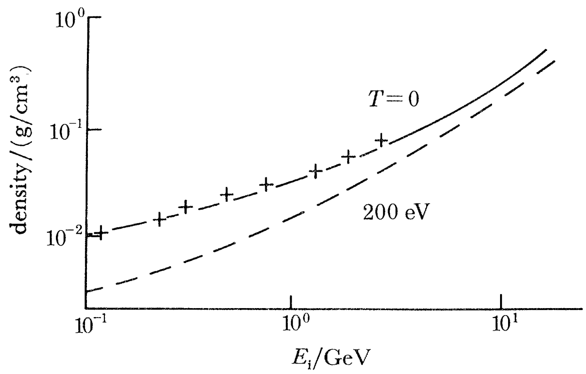

FIGURE 2. The variation with ion energy E_i of the range of uranium ions in cold gold at normal density (——) and in hot gold (T = 200 eV) at one-hundredth normal density (– – –). Also shown are the ranges from the Northcliffe & Schilling (1970) compilation (+).

and $\epsilon(\omega)$ is the complex dielectric constant of the plasma; fn and $h\omega_n$ are respectively the oscillator strengths and energies of levels of the atoms; ω_p is the classical bulk plasma frequency of the bound electrons. C/Z_2, where Z_2 is the atomic number of the slowing-down medium, represents an empirical shell correction which must be included when considering the behaviour of ions, particularly light ions, which have attained energies less than a few megaelectronvolts per atomic mass unit (Bischsel 1972; Bonderup 1967; Walske 1952, 1956). Equation (5) is, strictly, only applicable to cold materials and allowing $\omega_p \to 0$ and $\delta \to 0$ produces the familiar Bethe–Fano expression with no polarization correction due to the material density effects. Central to the application of (5), particularly for partially ionized plasmas, is the evaluation of the mean ionization potential I. Extending the earlier arguments of Bloch (1933), who used the Thomas–Fermi model to show that for $Z_2 \gtrsim 20$ (the range of applicability of the standard Thomas–Fermi model), $I/Z_2 \approx$ const., Ball *et al.* (1973) found that $I/Z_2 \approx 5$ eV, a result which agrees with experimentally determined values to no better than about a factor of two. An effective mean ion equation of state with suitable screening parameters is required that should be consistent with the degeneracy limit of the Thomas–Fermi model (Layzer 1959; Shalitin 1965). As the free electron density increases with temperature, an additional component $S_p(E_i)$ must be added to (5), representing the binary and collective slowing-down of the projectile ion with the free electrons. $S_p(E_i)$ may be calculated by standard dielectric theory (see, for example, Sigmar & Joyce 1971, Nardi *et al.* 1978). Since the free electrons ($S_p(E_i)$) will generally have a larger impact parameter than the bound electrons ($S_b(E_i)$), a range shortening can be expected with increasing temperature. This is illustrated in figure 2 where the range of 1–10 GeV U ions in gold is shown, first for cold ($T = 0$) gold at normal solid density and secondly for hot gold ($T = 200$ eV) at one-hundredth of normal density to approximate the effect of the ablator expansion in a pellet. A factor of about two occurs in the range shortening. Also shown on the figure are the ranges in the Northcliffe & Schilling (1970) compilations, although it should be stressed that these are data extrapolated from lower energy measurements. It should be noted that it may be necessary to add a small correction to (5) allowing for nuclear Coulomb scattering of the projectile ion at the end of its range.

A particularly important point in computing $S(E_i)$ is the value of Z_i that must be used, that is the effective charge state of the projectile ion as it slows down. Entering the plasma in a low charge state the ion will rapidly strip electrons (via plasma–electron and ion–electron impacts) until there is insufficient energy in the ion coordinate system to strip any more. The ion will then accrue electrons so that its effective charge decreases, according to Betz (1972), as

$$Z_i = Z_{\text{eff}} = Z_0\{1 - C(0.71 Z_0^{\alpha})^{v/v_0}\}, \quad v \gtrsim v_0, \tag{6}$$

where Z_0 is the number of protons in the projectile ion, C and α are experimentally obtained constants, and $v_0 = 2.188 \times 10^8$ cm/s is the Bohr velocity. According to Betz the form of (6) is applicable over a wide range of cold materials, the values of α and C being only weakly dependent on the choice of material. The effective charge predicted is usually within one or two charge units of the measured values. Using (6) for a 10 GeV U ion yields $Z_{\text{eff}} = 0.98 Z_0$. Calculations by Beynon & O'Dwyer (unpublished) show that a U^{2+} 10 GeV ion will reach a maximum stripped state of $Z_{\text{eff}} \approx 0.9\, Z_0$ in a time of less than 10^{-13} s, in reasonable agreement with the Betz prediction. The effect of (6) on computing $S(E)$ will generally be to flatten the Bragg peak in the dE/dx against x curve with a subsequent net small increase in the range of the ion. It should be remembered that (6) is strictly applicable to cold materials only since measurements have yet to be made in the material temperature and density, and energy ion range relevant to i.c.f.

It should also be stated that of equal importance to the above interaction physics is a proper representation of the effects on the energy deposition profile in the target of the geometry of the ion beams incident on the target and of the energy distribution within a beam.

3.3. *Non-elastic and other competing reactions*

In addition to the elastic Coulomb interactions outlined above there are a number of other interactions that the projectile ion will undergo during its slowing down in the target plasma. For the range of particle mass and energy central to ion-driven fusion we shall see that these effects are, if not negligible, at least small.

First, if we examine the energy loss of the projectile ion by bremsstrahlung radiation it is easily shown (Jackson 1975) that the ratio of this energy loss to collisional loss, $\Delta E_b/\Delta E_c$, is given by

$$\Delta E_b/\Delta E_c \approx \tfrac{4}{3}\pi^{-1} Z_1^2 Z_2/137)(m/M_i)\,\beta^2 L, \; \beta < 1,$$

where $L = \ln(2mc^2\beta^2\gamma^2/I) - \beta^2$.

Thus for a fully stripped 10 GeV U ion in solid gold ($I \approx 750$ eV.)

$$\Delta E_b/\Delta E_c \approx 1.9 \times 10^{-3},$$

while bremsstrahlung production by the scattered electrons can be shown to be negligibly small for $\beta \lesssim 0.9$ (Jankus 1953). Energy loss by pair production (electron–positron) ΔE_p, will only be significant in the ultra-relativistic limit when

$$\Delta E_p/\Delta E_b \approx (M_i/mZ_i^2) \times 10^{-3} \ll 5\,\%, \quad \gamma > 1,$$

energy loss by pion production being an order of magnitude less than this. Moreover, only at $\gamma \gg 1$ will the structure of the projectile ion need to be considered.

A problem of more importance is that of hadronic interactions of the projectile ions with the ions in the target plasma. Assuming a hard-sphere cross section between A_1 and A_2 of $\sigma = \pi(R_1 + R_2 - 2\Delta)^2$ where $R_i = 1.45A_i^{\frac{1}{3}} \times 10^{-13}$ cm and $\Delta \approx 0.85 \times 10^{-13}$ cm, we obtain $\sigma \approx 8b$ for a uranium ion interacting with gold. The probability of an ion with a Coulomb range of λ having *at least* one hadronic collision with ions of mass A_2 is $1 - \exp\{-\sigma A_0 \lambda / A_2\}$ where A_0 is the Avogardo constant. For 10 GeV U-ions in gold, if we assume $\lambda \approx 2 \times 10^{-1}$ g/cm^2, this probability is about 5×10^{-3}. Such interactions could have two effects. First, scattered ions, particularly light ions, would undergo medium to large angle deflexions, at the end of their range. Such effects would need to be included in a proper multiple scattering treatment, along with large angle Coulomb interactions. Secondly, the interaction may result in a fragmentation of the projectile ion and the target ion. The most likely effect is fission which, for the case of $A_1 \gg A_2$, will produce energy fragments of varying Z^2/E signature, resulting in differing ranges. Calculations of this effect for U ions in silicon show that there is an increased range of the ion beyond the Bragg peak of about 50 % but containing only about 10 % of the total energy deposited. Typically about 5 % of the U ions undergo such interactions. An assessment of the importance of this effect will depend on the particular target structure and ion beam considered but would certainly need to be included in a comprehensive treatment of the physics of the ion–plasma interaction.

3.3. *Summary*

It is probably true to claim that calculation of energy–range relations for energetic ions in cold materials give results in reasonable agreement with measured values. There are however few data above about 10 MeV/u and most compilations rely on extrapolations into this energy range (cf. Barkas & Berger 1967; Northcliffe & Schilling 1970). Some recent range measurements by Tarlé & Solarz (1978) on ^{56}Fe nuclei at 600 MeV/u show discrepancies of about 3 % with Barkas–Berger predictions which use the Bethe–Fano formalism with shell effect and density corrections. It should be noted that the Bethe–Fano formalism is a first Born quantum-mechanical theory and consequently some care should be exercised in using it for high charge state relativistic ions. In this case high-order corrections to the Mott cross section (Ahlen 1978) should be applied. In the Tarlé–Solarz work, for example, these corrections bring the agreement of measurement and calculation to within about 1%. In partially ionized hot plasmas no data are yet available and because of the uncertainties associated with the effective charge state of the ion and the mean ionization potential *I*, the ranges are probably not known to better than a factor of two. More measurements in both cold and hot materials are clearly required.

4. Production and transport of intense ion beams

In this concluding section an outline is presented of some of the current thinking on the production and the transport of intense ion beams to target pellets.

4.1. *Heavy ion accelerators*

Feasibility studies, both experimental and theoretical, are currently being made of a range of possible low-β accelerator types to find a suitable heavy ion driver. The final system must have a peak power output between 100–200 TW, a delivered energy of 1–10 MJ for $A \gtrsim 100$, at energies between 1–10 GeV with repetition rate of 5–15 Hz. The leading contenders are the r.f. linac and the induction linac although possible contenders include the synchrotron–storage ring systems and collective ion accelerators (Vesker & Budker 1956; Destler *et al.* 1980). The r.f. linac concept is based on the fact that a single r.f. linac can accelerate only small currents and therefore requires storage rings for use as a driver. Consequently a tree of r.f. linacs is envisaged which increases the frequency and intensity of the beam in steps as the beam energy increases. The resulting accelerated beam current is finally increased, and the final pulse length decreased, in storage rings and buncher systems. Severe problem are associated with the matching of the low velocity end of the r.f. machine into the high frequency sections, and with the beam emittance growth due to the strong space-charge forces at these currents. Induction linac concepts, on the other hand, use a single pass mode with gradual pulse-length compression during acceleration with a resulting inherent simplicity of beam handling in the absence of storage ring requirements. However considerably more experimental experience with heavy ions is required before the induction linac concept acquires the same level of confidence as the r.f. linac scheme.

Problems associated with storage ring design include the instability associated with resistive coupling of the beam to the walls of the beam vacuum chamber, intra-beam charge exchange, and the scattering of ions off the background gas. At the Berkeley Heavy-Ion Workshop in 1979 no serious flaws were found to discourage continued development of heavy ion drivers for fusion, and several test bed facilities are planned or nearing completion at the Argonne National Laboratory, the Brookhaven National Laboratory, the Lawrence–Berkeley Laboratory and the Los Alamos Scientific Laboratory.

4.2. *Light ion drivers*

Production of terawatt light ion beams (protons, deuterons, etc.) is based on the use of magnetically insulated small-area diodes (of about 10 cm^2) to generate currents of megamps at energies of megaelectronvolts. In the magnetically insulated diode a magnetic field, produced either externally or by the currents in the diode, is used to insulate electrons by inhibiting their motion from cathode to anode. The electrons flow along magnetic field lines forming a virtual cathode opposite the anode. This results in a larger portion of the diode current flowing as ions. By insulating the electrons thus from the anode and using a virtual cathode rather than a physical metal one, diode damage can be significantly reduced and repeated firing of such diodes can be achieved with little maintenance. Discussion of the technology of these devices, including the design of the higher power pulse-forming lines, is outside the scope of this paper but the reader is referred to the paper by Martin *et al.* (1979) and other papers at the 1969 Novosibirsk meeting. It is worth recording that the 30 TW, 1 MJ light ion accelerator PBFA-I is expected to become operational at the Sandia Laboratories during the summer of 1980.

4.3. *Beam propagation to target*

Common to both light and heavy ion drivers is the problem of the stable propagation and focusing of an intense ion beam to a small target, of dimensions of a few millimetres. Three possible modes of propagation have been considered, namely ballistic propagation, self-focused propagation and pre-formed channel propagation. Ballistic focusing for heavy ions, because of the lower current requirements, is an approach for which no new concepts are needed. At reactor chamber pressures less than about 0.2 Pa the mean free path for ionization is greater than the reactor chamber dimensions, and the final spot size is determined by space-charge variations and aberrations in the focusing system. Increasing the chamber pressure results in plasma focusing and stripping, electro-magnetic and electrostatic instabilities, and possible beam deflexions due to the magnetic fields generated by the knock-on electrons. In the self-focused mode the reactor chamber is at a pressure in excess of 200 Pa with a beam radius pre-focused by the chamber to be equal to the target size. Expansion and energy loss occur at the front of the beam in the initially neutral gas, while charge neutralization and partial current neutralization occur behind the beam front. An equilibrium radius is believed to occur when the residual self-magnetic field of the beam balances against the beam internal pressure. In the preformed channel mode, which has received detailed study for light ion propagation, an azimuthal self-magnetic field of a preformed current channel is balanced against the beam pressure to provide equilibrium at chamber pressures in excess of about 200 Pa. Questions remain, however, regarding the stability of this mode.

5. Concluding remarks

There is as yet no clear cut choice emerging for a light or heavy ion driver. The euphoria of three or four years ago has diminished as the physics and technological problems have presented themselves more clearly. However the high efficiency of accelerator driver systems make their possible use for i.c.f. power stations more attractive than any other driver system so far considered.

References (Beynon)

Ahlen, S. P. 1978 *Phys. Rev.* A **17**, 1236.
Allison, S. K. & Warshaw, S. D. 1953 *Rev. mod. Phys.* **25**, 779.
Ball, J. A., Wheeler, J. A. & Fireman, E. L. 1973 *Rev. mod. Phys.* **45**, 333.
Barkas, W. H. & Berger, M. J. 1967 *Penetration of charged particles in matter*, paper 7. Washington D.C.: National Academy of Sciences–National Research Council.
Bethe, H. & Ashkin, J. 1953 *Experimental nuclear physics*. New York: Wiley.
Betz, H. D. 1972 *Rev. mod. Phys.* **44**, 465.
Bichsel, H. 1968 *Radiation dosimetry I.* New York: Academic Press.
Bichsel, H. 1972 *A.I.P. handbook*, pp. 8–142. New York: McGraw-Hill.
Bloch, F. 1933 *Annln Phys.* **16**, 285; *Z. Phys.* **81**, 363.
Bonderup, E. 1967 *K. danske Vidensk. Selsk. Mat. Fys. Medd.* **35**, 17.
Butler, S. & Buckingham, M. 1962 *Phys. Rev.* **126**, 1.
Destler, W. W., Floyd, L. E. & Reiser, M. 1980 *Phys. Rev. Lett.* **44**, 70.
Fano, U. 1963 *A. Rev. nucl. Sci.* **13**, 1.
Jackson, J. D. 1975 *Classical electrodynamics* (2nd edn). New York: Wiley.
Jankus, V. Z. 1953 *Phys. Rev.* **90**, 4.
Landau, L. N. & Lifshitz, E. M. 1960 *Electrodynamics of continuous media*. Reading, Mass: Addison-Wesley.
Layzer, D. 1959 *Ann. Phys.* **8**, 271.
Lindhard, J. 1954 *K. danske Vidensk. Mat. Fys. Medd.* **28**, no. 8.
Longmire, C. 1963 *Elementary plasma physics*. New York: Wiley.
Martin, T. H., Vandevender, J. P., Barr, G. W. & Johnson, D. L. 1979 *3rd International Topical Conference on High Power Electron and Ion Beam Research, and Technology, U.S.S.R.*
Nardi, E., Peleg, E. & Zinamon, Z. 1978 *Physics Fluids*, **21**, 574.
Northcliffe, L. C. 1963 *A. Rev. nucl. Sci.* **13**, 67.
Northcliffe, L. C. & Schilling, R. F. 1970 *Nucl. Data* A **7**, 233.
Rossi, B. 1952 *High energy particles*, ch. 2. Englewood Cliffs; New Jersey: Prentice-Hall.
Shalitin, D. 1965 *Phys. Rev.* A **140**, 1857.
Sigmar, D. & Joyce, G. 1971 *Nucl. Fus.* **11**, 447.
Sternheimer, R. M. 1956 *Phys. Rev.* **103**, 511.
Tarlé, G. & Solarz, M. 1978 *Phys. Rev. Lett.* **41**, 483.
Uehling, E. A. 1954 *A. Rev. nucl. Sci.* **4**, 315.
Vesker, V. I. & Budker, G. I. 1956 In *Proceedings of the CERN Symposium on High energy Accelerators*, Geneva; see also *At. Energy* **1**, 9 (1950).
Walske, M. C. 1952 *Phys. Rev.* **88**, 1283.
Walske, M. C. 1956 *Phys. Rev.* **101**, 940.

Discussion

A. C. Walker. (*Culham Laboratory, Abingdon, Oxfordshire OX*14 3*DB, U.K.*). Dr Beynon describes the rapid stripping of the ions as they enter the target pellet. If thin foils are used to separate the ultra-high vacuum of the accelerator from the reaction chamber, how serious is the problem of stripping of the ions within these foils – given that they have to be reasonably thick to stand the pressure fluctuations of the reactor and that more highly charged ion beams are more difficult to transport and focus?

T. D. Beynon. There is considerable discussion currently on the best method of propagating the ion beam from the final focusing magnet across the reactor chamber to the target, and current thinking on this subject is outlined in the final section of my paper. It is by no means obvious that thin foils need to be used to separate the vacuum of the accelerator from a reactor chamber which may be at a pressure of less than 5×10^{-4} Torr ($\approx 6.7 \times 10^{-2}$ Pa) if the ballistic propagation approach is adopted. Differential pumping across a multiple chamber geometry could be adequate. Alternatively, neutralized beam propagation in a ultra-high vacuum chamber could be used if an unfavourable charge state resulted from the use of such thin foils. This approach is currently being considered for light ion drivers.